Global Journal of Environmental Science and Management
(GJESM)

Homepage: https://www.gjesm.net/

Podcasts

ORIGINAL RESEARCH ARTICLE

Environmentally friendly synthesis of nanoporous silica materials using quercetin as a morphogenetic agent

A.R. Zare Hoseinabadi[1], E. Rafiei Taqanaki[1], S. Hafez Ghoran[1], A.M. Amani[1], H. Kamyab[2,3,4,*], A. Razmfarsa[5], E. Khalili[6], M. Yusuf[7,8], S. Rajendran[9]

[1] *Department of Medical Nanotechnology, School of Advanced Medical Sciences and Technologies, Shiraz University of Medical Sciences, Shiraz, Iran*

[2] *Faculty of Chemical and Energy Engineering, Universiti Teknologi Malaysia, 81310, Skudai, Johor, Malaysia*

[3] *Universidad UTE, Centro de Investigación en Salud Públicay Epidemiología Clínica, Quito 170527, Ecuador*

[4] *Department of Biomaterials, Saveetha Dental College, and Hospital, Saveetha Institute of Medical and Technical Sciences, Chennai, 600 077, India*

[5] *Faculty of Science, Department of Biology and Genetics, Islamic Azad University, Mashhad Branch, Razavi Khorasan, Iran*

[6] *Department of Electrical and Engineering, Faculty of Engineering and Physical Science, Centre of Vision Speech and Processing, University of Surrey, United Kingdom*

[7] *Clean Energy Technologies Research Institute, Process Systems Engineering, Faculty of Engineering and Applied Science, University of Regina, Canada*

[8] *Centre of Research Impact and Outcome, Chitkara University Institute of Engineering and Technology, Chitkara University, Punjab, India*

[9] *Instituto de Alta Investigación, Universidad de Tarapacá, Arica 1000000, Chile*

ARTICLE INFO

Article History:
Received 02 May 2024
Revised 27 July 2024
Accepted 02 October 2024

Keywords:
Antioxidant properties
Antiviral assay
Cell viability
Mesoporous silica nanoparticles
Quercetin
Templating technique

ABSTRACT

BACKGROUND AND OBJECTIVES: The synthesis of mesoporous silica nanoparticles using non-surfactant agents is gaining popularity owing to the easier purification and lower toxicity of this method compared to traditional surfactant-based ones. The potential of mesoporous silica nanoparticles as advanced nanocarriers for health-related applications is increasingly recognized. Quercetin, a potent free-radical scavenging antioxidant that relies heavily on the intracellular supply of reduced glutathione, has garnered significant interest in the scientific community. In spite of recent progress, the mechanisms underlying the development of the porous framework have largely gone unexplored. The primary aim of this study is to explore the feasibility of utilizing quercetin as a template for the synthesis of mesoporous silica nanoparticles, circumventing the need for conventional
METHODS: This research investigates the impact of the chemical structure and properties
METHODS: This research investigates the impact of the chemical structure and properties of polyphenols, specifically quercetin, on their templating potential. The study reveals the arrangement of quercetin, which acts as a model for the development of mesoporous silica nanoparticles, forming a supramolecular structure that facilitates silica binding. The composition of this supramolecular framework leads to unconventional and variable pore structures. The scanning electron microscopy, transmission electron microscopy, Fourier-transform infrared spectroscopy, x-ray diffraction analysis, energy-dispersive X-ray spectroscopy, and Brunauer–Emmett–Teller analysis were used to characterize the quercetin-templated mesoporous silica nanoparticles and provide detailed insights into their morphology.
FINDINGS: The results from the viability test and antiviral assays demonstrated that quercetin-templated mesoporous silica nanoparticles are non-toxic and possess inhibitory and antiviral properties that are comparable to those of Oseltamivir, which served as a positive control. Quercetin served as a non-surfactant, neutral template in an ammonia and ethanol mixture, resulting in approximately spherical particles with monodisperse diameters of about 180 nanometers. These nanoparticles of mesoporous silica showed a concentration-dependent efficacy in inhibiting pathogenic microorganisms. In x-ray diffraction pattern for Mesoporous silica nanoparticles, a number of Bragg's reflections referring to the (111), (200), and (220) sets of lattice planes were detected, which can be described by the fundamental face center cubic structure of mesoporous silica nanostructures. Because of the smaller particle diameter impact and incomplete internal structure of the nanostructures, the intense peak at 2θ= 24 degrees demonstrated the silica peak, which reflected crystalline nature. According to calculations based on the Brunauer–Emmett–Teller method, the specific surface area of Quercetin-templated mesoporous silica nanoparticles was determined to be 55.227 cubic meters. Furthermore, the Barrett-Joyner-Halenda analysis provided measurements of the pore size at 24.312 nm and the pore volume at 0.336 square centimeters per gram, respectively.
CONCLUSION: The study results outcomes demonstrated that quercetin forms a macromolecular scaffold that functions as a template for the formation of mesoporous silica nanoparticles. The irregular pore structure observed is attributed to the unique characteristics of quercetin. Using small-angle x-ray scattering, detailed information was obtained regarding the constituents and the porous nature of the resulting mesoporous silica nanoparticles. This study reveals innovative insights into the mechanisms by which the macromolecular structure of the template governs the dimensions of particles and the process of pore formation. The role of quercetin in the morphogenetic development of mesoporous silica nanoparticles has been thoroughly investigated. In addition, quercetin-templated mesoporous silica nanoparticles exhibited significant antioxidant properties, akin to butylated hydroxytoluene, and showed great potential for various clinical applications.

DOI: 10.22034/gjesm.2024.10.SI.09

This is an open access article under the CC BY license (http://creativecommons.org/licenses/by/4.0/).

NUMBER OF REFERENCES
40

NUMBER OF FIGURES
9

NUMBER OF TABLES
0

*Corresponding Author:
Email: *hesam_kamyab@yahoo.com*
Phone: +6017 782 0054
ORCID: 0000-0002-5272-2297

Note: Discussion period for this manuscript open until November 1, 2024 on GJESM website at the "Show Article".

INTRODUCTION

Mesoporous silica nanoparticles (MSNs) are gaining popularity because of their large surface area and tunable pore size, hydrophilicity properties, quick and efficient surface modification, and biocompatibility specifications. These characteristics are highly desirable for a variety of applications, such as medication delivery, catalysis, imaging, and sensing/detecting (Abbasi *et al.,* 2021, Vafa *et al.,* 2021, Vafa *et al.,* 2022). The realization of this promise necessitates the use of monodisperse mesoporous silica nanoparticles (MSNs) measuring between 50 and 200 nanometers (nm) to improve cellular uptake, as well as possessing large mesopores to allow for the encapsulation of biomacromolecules, particularly within the biomedical sector (Gao and Zharov, 2014; Vafa *et al.,* 2023). Natural resources containing silica are more considered because of their low cost, biocompatibility, bioactivity, and bioavailability. Furthermore, for these purposes, the intrinsic capacity generated by interconnected pores will be valuable, and it can be caped using different materials and decapped under special conditions such as the acidic potential of hydrogen (pH). Surfactant templating has become the most popular method for synthesizing MSNs. In 1992, it was discovered that when surfactant molecules self-assemble in the aqueous systems of silica substances, spontaneous silica-surfactant mesophase co-assembly would occur (Kresge *et al.,* 1992). Following the removal of the surfactant, the resultant composition includes relatively standard solids of the mesoporous matrix, as well as the hazardous replication of the supramolecular structures that were self-assembled by the surfactant. A broad range of compositions of mesoporous solids have been developed in recent years (Fröba *et al.,* 1999; Stevens *et al.,* 2006; Zhao *et al.,* 1998), and the ability to tune porous structure dimensions from one to tens of nanometers has been illustrated by leveraging a range of surfactants. Using templating chemicals, typically surfactants, a variety of techniques for mesoporous silica nanoparticles (MSNP) production have been established (Han and Che, 2013). Wei *et al.* (1998) maintained that, decades later, homogenous silica with a mesoporous matrix might well be manufactured by employing D-maltose, D-glucose, and dibenzoyl-L-tartaric acid, resurrecting the application of nonsurfactant substances as templating agents. Other chemicals, including organic hydroxy-carboxylic acids, poly(propylene)imine dendrimers (like lactic acid, tartaric acid, malic acid, and citric acid), complexes of the β-cyclodextrinurea-urea, and sugars (like fructose and sucrose), were found to be effective in generating mesoporous silica monoliths in corresponding tests (Pang *et al.,* 2001a; Pang *et al.,* 2001b; Vafa *et al.,* 2024; Wei *et al.,* 1999; Zheng *et al.,* 2002). Subsequently, the technique was effectively utilized for the synthesis of nanostructures. Although the diameter of nonsurfactant-based templated MSNs may differ without losing monodispersity, owing to the limited scale of the templating species, the pore diameter becomes typically less than 4 nm (Gao and Zharov, 2014). Plants that possess a significant concentration of polyphenols often display complex structural arrangements. In this framework, phenolic rings serve as the essential monomers, which are further classified into phenolic acids and phenolic alcohols (Abbas *et al.,* 2017; Amani *et al.,* 2024). A revolutionary technique for creating mesoporous silica nanostructures with accurate pore volume spatial distribution, high surface area, and adjustable pore diameters is the green template. It has been demonstrated that this template can be completely removed and recycled from silica sustainably by quickly eliminating water. In addition, the porous structure has a high thermal resistance (Luo *et al.,* 2019; Xu *et al.,* 2008). An abundant flavonoid antioxidant agent found in nature is quercetin (QU). The extensive array of functions it exhibits, including the modulation of cell growth and engagement through type II estrogen binding sites, positions it as a highly promising candidate for the advancement of anti-tumor therapies. However, tyrosine kinase inhibition is typically present as a glycoside that, during intestinal absorption, transforms into glucuronide/sulfate conjugates. Furthermore, the circulatory system uses only conjugate derivatives. Previous research has shown that QU can cure metabolic ailments, allergy syndromes, eye issues, arthritis, and heart failure. Moreover, it is a strong antioxidant that protects against tissue deterioration over time brought on by a range of medication toxicities (David *et al.,* 2016; Lakhanpal and Rai, 2007). Some plants containing high levels of polyphenols possess complicated structures. In this respect, the basic monomer is a phenolic ring that is classified into phenolic acids and phenolic alcohols (Abbas *et*

al., 2017; Amani *et al.,* 2024). The green template strategy has emerged as a groundbreaking method for generating mesoporous silica nanostructures, enabling the manipulation of pore diameters, the accurate spatial distribution of pore volume, and the attainment of a significant surface area. It has been shown that by rapidly extracting water, this template can be fully removed and recycled from silica in an environmentally friendly manner. Aside from that, the porous structure is very thermally resistant (Luo *et al.,* 2019; Xu *et al.,* 2008). QU is a flavonoid antioxidant agent abundantly available in nature. A large percentage of its behaviors, including cell growth regulation and interaction through type II estrogen binding sites, make it a potential anti-tumor drug applicant. Nevertheless, tyrosine kinase inhibition is commonly found as a glycoside, which is converted to glucuronide/sulfate conjugates during gut absorption. Moreover, only conjugate derivatives are used in the circulatory system. QU has been demonstrated to reduce the risk of heart failure and cure eye disorders, arthritis, allergic syndromes, and metabolic diseases in previous studies. It is also a potent antioxidant that has been noticed to defend against tissue long-term damage caused by a variety of drug toxicity (David *et al.,* 2016; Lakhanpal and Rai, 2007). The aim of this study is to explore the environmentally friendly synthesis of MSNs using QU as a non-toxic morphogenetic agent. By investigating the templating potential of QU, the research seeks to elucidate the structural characteristics and mechanisms underlying the formation of unique porous frameworks in MSNs. The study centers on the characterization of the resultant nanoparticles, alongside an assessment of their biocompatibility and prospective biomedical applications, particularly in drug delivery and antimicrobial activities. Ultimately, the findings could contribute to the development of safe and effective nanocarriers for health-related purposes, advancing the understanding of polyphenol-assisted synthesis in nanotechnology. This study has been carried out in Iran in 2024.

MATERIALS AND METHODS

Sigma-Aldrich provided tetraethoxysilane (TEOS), concentrated 28 percent % ammonium hydroxide, QU, absolute ethanol, concentrated 30% hydrogen peroxide, and concentrated 98% sulfuric acid. All of these materials were used as acquired.

Silica nanoporous material synthesis

QU was used as a templating agent throughout the production of nanoporous silica particles, and it was dissolved in 150 mL of ethanol before being applied to a mixture of ammonia and water. Following the synthesis process, the particulates were collected through centrifugation and subsequently subjected to thorough washing with water and ethanol prior to their redispersed. The residues of the organic compounds were removed using an acid piranha procedure. To eliminate all of the ethanol, 0.1 gram (g) of particulates were distributed throughout the water multiple times. The resulting aqueous solution was treated for 2 hours (h) at 60 degrees Celsius (°C) using a diluted piranha solution, consisting of 10% hydrogen peroxide (H_2O_2) and 2 molar sulfuric acid (H_2SO_4), while stirring the mixture. The process was completed after centrifuging the suspension for 10 minutes at 7800 Revolutions per minute (rpm). To ensure the removal of acidic substances, the particulates were washed three times with water prior to their re-dispersion in the aqueous solution.

Characterization

Scanning electron microscopy (SEM) was performed using the Hitachi S-4800 equipment. In addition to assessing the silica particle properties, SEM was used to investigate the QU aggregates. SEM was used to determine the median size and distribution of the associated nanostructures. Transmission electron microscopy (TEM) was performed using the JEOL JEM instrument, 2200fs model. Nitrogen adsorbents were employed to assess the surface area and volume of the porous structures present in crystalline silica. At 77 K, nitrogen desorption and adsorption processes were quantified using the micromeritics triflex. The Brunauer-Emmett-Teller (BET) method was also employed to determine the unique surface area. In addition, small angle X-ray scattering (SAXS) analysis methods were used to determine the pore diameter and surface unevenness of the particles. X-ray photoelectron spectroscopy (XPS), which is used to detect empirical atomic properties and chemical composition, was employed in this study to investigate the molecular structure of the chemical configuration and the electronic institution of the components inside the sample. The development of Fourier transform infrared (FTIR) spectroscopy as an experimental analytical method allows for

the differentiation of organic materials from certain inorganic substances through the use of infrared radiation (IR). The X-ray diffraction (XRD) test was used as a non-destructive evaluation method to determine the composition of crystalline phases and structures present in these nanostructures.

Antioxidant assay

The antioxidant ability of QU-synthesized MSNs was determined on the basis of scavenging the free radicals, 2,2-diphenyl-1-picrylhydrazyl (DPPH•), using a spectrophotometric assay (Ghoran *et al.,* 2020). The different concentrations of MSNs were employed in the range of 62.5-100 microgram per mL (µg/mL) (Loizzo *et al.,* 2012). Butylated hydroxytoluene (BHT) was used as a positive control. After having incubated for 30 minutes at 37 °C, absorbance at 517 nm was measured. The percentage inhibition of DPPH• radical formation was measured using Eq. (1) (Loizzo *et al.,* 2012):

$$\text{DPPH scavenging effect}(\%) = \left[\left(\text{A0} - \text{A1}\right)/\text{A0}\right) \times 100] \quad (1)$$

where A_0 is the absorbance of the control reaction, and A_1 is the absorbance of the presence of all the extract samples and standard.

Antibacterial assay

In this study, two bacterial species were used in the inhibition zone, i.e., minimum bactericidal concentration (MBC) and minimum inhibitory concentration (MIC) tests. *Escherichia coli* (ATCC8739) and *Staphylococcus aureus* (ATCC6538) were used as bacterial strains in the investigation. The medium of lactose broth (LB) and fresh nutrient broth (NB) was given to *E. coli* and *S. aureus*, allowing them to develop for 24 to 48 h in a typical environment with 37 °C temperature. Serial dilution was used to produce different dilutions of each bacterial strain suspension. The amount of absorption was next evaluated by employing a spectrophotometer calibrated to 580 nm. Each bacterial suspension strain employed in previous comparable studies has been adjusted to have 0.5 normal McFarland turbidity.

Growth inhibitory zone determination

The growth inhibitor zone diameter of each sample was measured using a Disc Diffusion Protocol which was established initially in the 1940s and, since that time, has been further refined by the recommendations of the Clinical and Laboratory Standard Institute (CLSI) (Balouiri *et al.,* 2016). The bacterial solutions, *S. aureus* and *E. coli*, were individually grown at a 0.5 McFarland concentration (Mueller-Hinton agar). The discs soaked in various quantities of the sample (QU-templated MSNs) were then put on the culture medium at the appropriate distances. The experiment included a disc with penicillin as the positive control, alongside a chemically inert blank disc designated as the negative control. Following a 24-hour incubation at 37 °C, the diameters of the zones of growth inhibition were measured under suitable conditions. Both experimental procedures were repeated three times.

Minimum bactericidal concentration and minimum inhibitory concentration determination

The MBC and MIC of various nanostructures were determined using the tube dilution method. A tube was supplied separately with 9 mL of Mueller-Hinton Broth, 1 mL of a sample (QU-templated MSNs). The serial dilution method then produced different concentrations of each material. The suspension of the bacterial strain at 0.5 McFarland levels (0.1 mL) was combined in all tubes with the preceding combination. The tubes may be incubated overnight at 37 °C. The MIC was described as the lowest concentration during which the bacterial growth was stopped, without turbidity in tubes. The MBC was found to be the lowest nanomaterial level, producing a decrease of 99.9% of 10^8, 0.5 McFarland's standard (CFU/mL) in bacteria colonies from the original inoculum (Balouiri *et al.,* 2016). In this context, the medium tubes that are free of micro-organisms are designated as the negative controls, whereas the medium tube that includes micro-organisms without a sample is identified as the positive controls. The same technique has been used in conventional medicine for the comparison of antibacterial action with an antibiotic (penicillin). The experiments have been repeated at least three times to ensure reliability.

Cytotoxicity endpoints and cell culture

A cellular study was conducted using fibroblast cells. The fibroblast cell line was acquired from the National Cell Bank of Iran by the Pasteur Institute. The cell lines were produced in a flask of 5% carbon

dioxide (CO_2), 37 °C (Gibco, Scotland) of the RPMI-1640 medium with 10% of fetal bovine serum (FBS, PAA, Austria), and 1% penicillin/streptomycin. The cells were cultured in a flask. When the cells achieved a confluence of about 70–80%, they were washed with phosphate-buffered saline (PBS). The cells were then removed with trypsin/EDTA from the flask for a brief time. The evaluation of cell density was conducted utilizing a Neubauer chamber in conjunction with trypan blue staining of the harvested cells. The cytotoxicity of the produced sample (QU-templated MSNs) has been evaluated in various doses by using the mitochondrial dehydrogenase-dependent 3-4, 5-dimethylthiazolyl-2-2, and 5-diphenyltetrazolium bromide (MTT) assay (Twentyman and Luscombe, 1987). The cells cultured were seeded in 96-well cell cultures at a density of 1×10^5 cells per well. The cells were incubated at 5% CO_2 and 37 °C for 24 h. After the incubation period, the culture media was removed and the cells were incubated at different concentrations in the new medium for 24, 48, and 72 h (5, 10, 20, 50, 100, 150, 200, and 250 g/mL). Cells with no samples were negative controls. A 100 mL MTT dye solution was well received at a concentration of (0.5 mg/mL in PBS), then incubated for 3 h. Then, each cell received 100 mL of DMSO (Merck, Germany). A plate reader was used to evaluate 570 and 650 nm absorption (Perkin Elmer, Boston, USA). The cytotoxicity and viability of the cells were evaluated using the control group, which had 0 percent cytotoxicity volume and 100 percent viability volume. Cytotoxicity and viability percentages were measured for different sample concentrations using Eqs. (2) and (3), respectively (Luo *et al.,* 2019):

$$\text{Cell viability}(\%) = \frac{AbSt570 - AbSt650}{AbCon570 - AbCon650} \times 100 \quad (2)$$

$$\text{Cytotoxicity (\%)} = 1 - \text{cell viability (\%)} \quad (3)$$

where AbSt570 and AbSt650 have sample light absorption values of 570 and 650 nm, respectively, and AbCon570 and AbCon650 represent the light absorption of control samples.

Statistical analysis

All the tests were performed three times, and results were shown as the mean ± standard (SD). To monitor differences between variables, an analysis of variance (ANOVA) was conducted. The data were statistically examined using the Social Sciences Statistics Package (SPSS), version 20.0. (SPSS Inc. USA). For comparison, T-tests were employed. When the *P*-value was below 0.05, it was considered that statistically significant results were obtained ($P < 0.05$). All tests were performed three times.

RESULTS AND DISCUSSION

Amorphous silica is found in a variety of living organisms, including diatoms, silicoflagellates, radiolarians, and sponges (Maldonado *et al.,* 2005; Riesgo *et al.,* 2021). The structural configuration of molecules and atoms in amorphous silica, or non-crystalline silica, is defined by a disordered and chaotic organization, devoid of a regular pattern. Peak broadening was also linked to the formation of porous structures in another analysis. Another characterization analysis, like TEM and BET surface analyzer, can be used to prove this theory. The presence of non-crystalline frameworks owing to pore formation through the QU template is shown by the widening/stretching of the sample diffraction peaks. According to Kioni *et al.,* wide-angle x-ray diffraction exhibits an amorphous-like form, which correlates to the existence of large pores in the material (Kioni *et al.,* 2011). The crystalline structure of QU-templated MSNPs is determined using an X-ray diffraction pattern. The existence of silica nanoparticles can be determined using XRD analysis. The particulates are crystalline in nature, as can be seen in Fig. 1, indicating that silica has a porous composition. The pores formed within silica are responsible for the peak broadening of diffraction peaks in the QU–templated silica. In profile (Fig. 1), diffraction peaks broadened at around 2q= 22–24°, as in the diffraction pattern of the amorphous phase of silica. The sharp peak at 2θ= 24° displays the silica peak, which represents the crystalline nature of the nanostructures, because of the incomplete internal structure and lower particle diameter influence. Bragg's reflections pertaining to the (111), (200), and (220) sets of lattice planes are identified in the XRD pattern for MSNs. These reflections can be explained by the basic face center cubic (FCC) structure of mesoporous silica nanostructures.

A mesoporous silica nanoparticle is a specific kind of mesoporous silica nanostructured material featuring a hollow spherical shape. Fig. 2 shows an

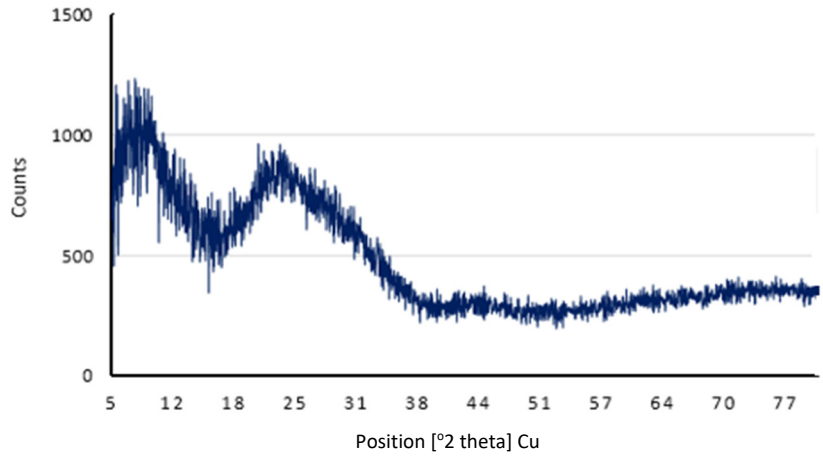


Fig. 1: Powder XRD pattern of synthesized QU-templated MSNPs.

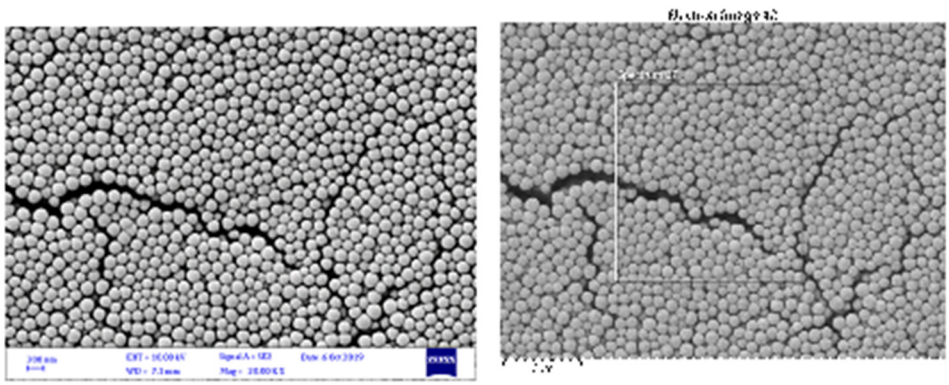


Fig. 2: SEM analysis of the synthesized QU-templated MSNs

SEM representation of QU-templated MSNs. TEOS as the silica precursor and cetyltrimethylammonium bromide (CTAB) as the pore-forming agent were used to produce QU-templated MSNs with a mean diameter of around 180 nm. The solid Stober spheres were effectively transformed into homogeneous hollow spheres when simply treated with sodium carbonate (Na_2CO_3) in the presence of CTAB at a sufficient concentration.

Fig. 3 shows the TEM images of QU-templated MSNs. The traditional SEM image of QU-templated MSNs shows spherical and monodisperse particulates, with a monodisperse particle having an average scale of 100–180 nm. The TEM image clearly shows that the QU-templated MSNs had a porous configuration with well-lined-up porous spherical arrangement and formed excellent nanoclusters. Sarkar *et al.* (2016) created MSN-Folic acid-quercetin as a targeted delivery system for breast cancer cells. The authors estimated the average diameter of MSNs to be 80–120 nm.

With nitrogen sorption measurement techniques, the dried nanostructure specimens were assessed for pore volume (V_p) as well as specific surface area (SSA_{BET}). The specific surface area was measured using the BET principle, and pore volume was calculated using the cumulative adsorbed quantity at a relative pressure of p/p_0 = 0.9 (Matshitse, 2010). Since the porosity variations between silica specimens were already apparent based on the various synthesis parameters, nitrogen sorption observations were taken for all porous silicon nanomaterial samples but only for one silica nano-sized sample. The N_2 adsorption/desorption isotherm models and the

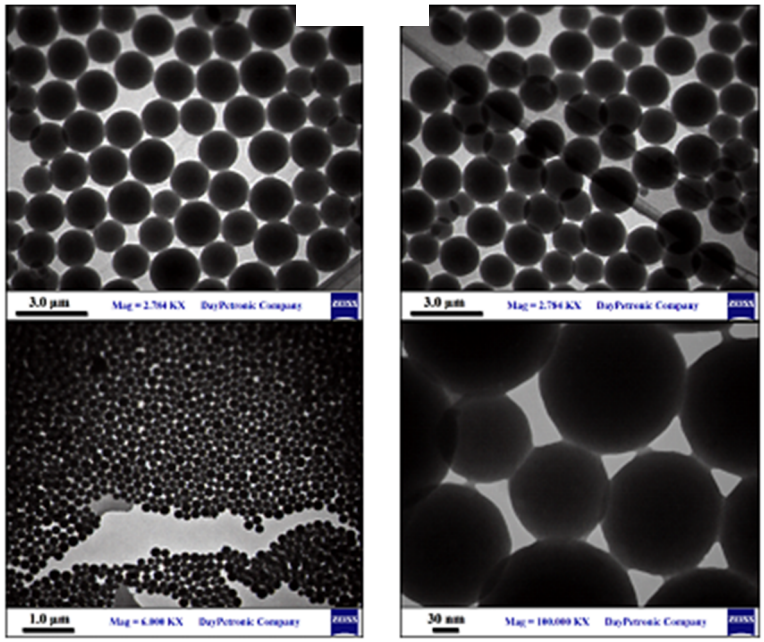


Fig. 3: TEM images of well-shaped monodisperse Quercetin-templated MSNs

pore size distribution of the QU-templated MSNs are seen in Fig. 4. The specific surface area of QU-templated MSNs was 55.227 m^2/g, according to BET surface area calculations, and the measured Barrett-Joyner-Halenda (BJH) pore size and pore volume were 24.312 nm and 0.336 cm^3/g, respectively (Fig. 4). The aminated MSNs provided a smaller surface area than the non-functional MSNs, meaning that the aminopropyl group effectively attached to the surface of the aminated MSNs. Because of the huge pore size and volume, these nanoparticles are predicted to have a special ability to load therapeutic agents.

FTIR was used to characterize the structures of QU-templated MSNs. The FTIR spectra of QU-templated MSNs are shown in Fig. 5. The characteristic peaks of about 1115 per centimeter (/cm), 874/cm, and 477/cm are recognizable in the spectra of silica nanostructures and are attributed to the asymmetric and symmetric stretching and bending vibrations of Si–O–Si, respectively, which is quite similar and in accordance with the study of Sarkar *et al.* (Sarkar *et al.,* 2016). The symmetric stretching of Si-OH generated a peak of about 1440/cm. In QU-MSNs, the carbonyl peak of quercetin shifted to 1619/cm because of the binding of MSN with QU. The stretching vibrations of Si-OH groups and QU were also correlated with the peaks of about 3414/cm (Nikolić *et al.,* 2010). The presence of crosslinked QU molecules was confirmed by the peaks in the QU-MSN areas of 2923, 2035, 1619, and 1384/cm, which correlated to aliphatic C–H vibrations and substituted-benzene groups, respectively.

With an EDS (Energy Dispersive X-ray Spectrometer) detector on the SEM, elemental analysis can be performed in addition to imaging the sample surface morphology and structure. The EDS spectrum of nanostructures prepared with QU as a pore-forming agent is shown in Fig. 6. As a result, a high-sensitivity EDS detector was used to trace the elemental EDX spectrum. The dominant constituents of the QU-templated MSNs, namely carbon ©, oxygen (O), nitrogen (N), iron (Fe), zinc (Zn), and silicon (Si), were successfully observed, and indications were employed for line scans and visualization. The binding energies of O and Si are represented by peaks of around 0.5 kV and 1.9 kV, respectively. The weight ratio of silica is 81.1%. The EDS spectrum's remaining lines correspond to the other elements (Au, Fe, and Zn).

Biocompatibility and antibacterial activity of QU-templated MSNs

There was no requirement to extract residual

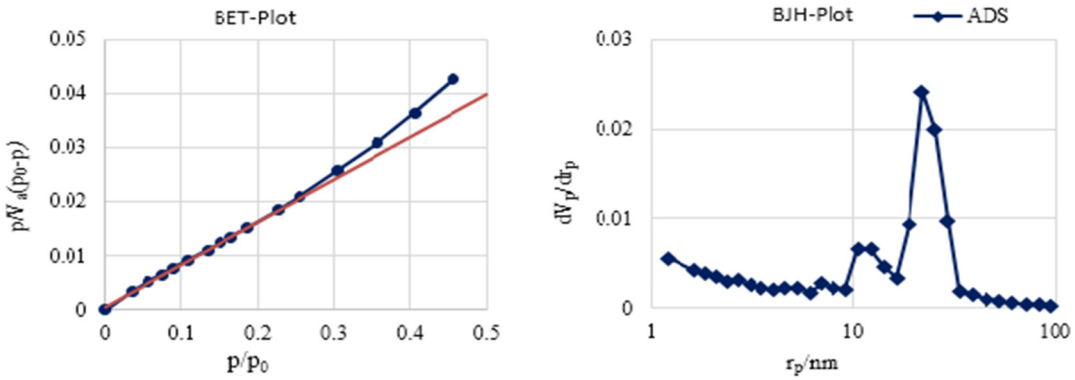


Fig. 4: The QU-templated MSNs pore diameter distribution and N_2 adsorption/desorption isotherm models

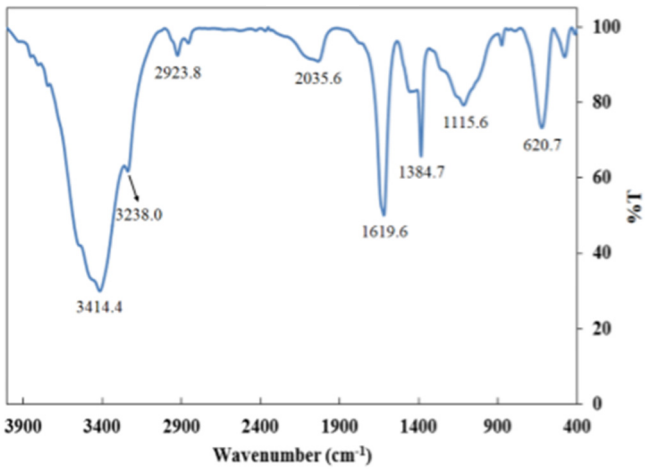


Fig. 5: FTIR spectra of QU-templated MSN

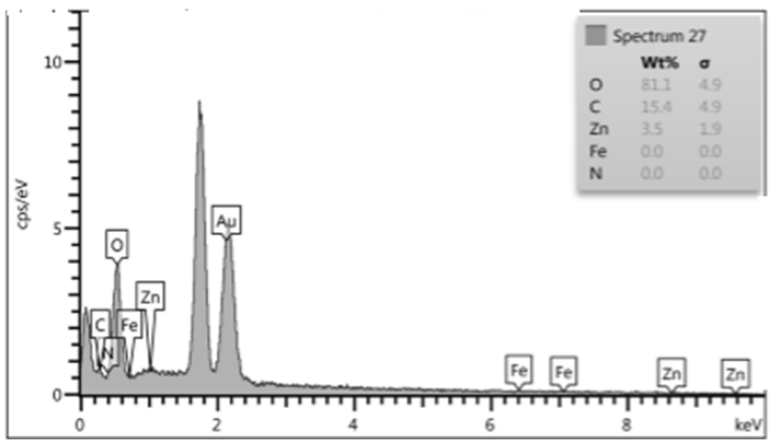


Fig. 6: EDS analysis of synthesized QU-templated MSs

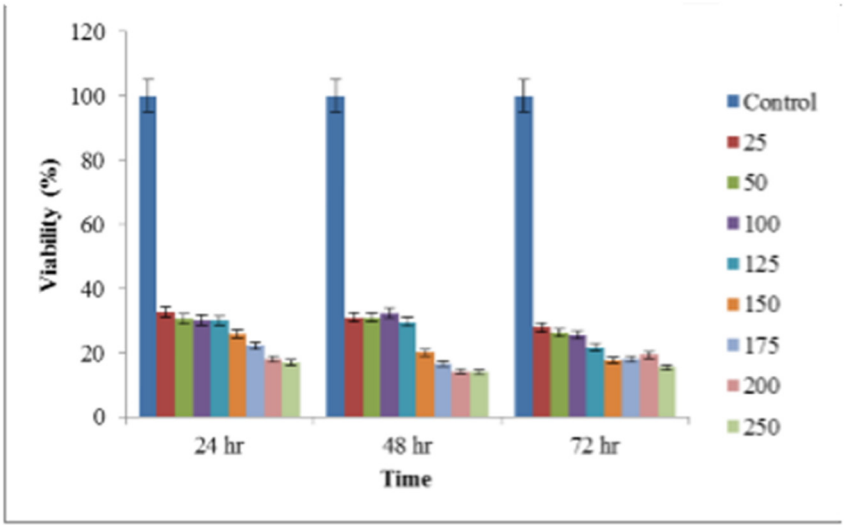


Fig. 7: Cytotoxicity of QU-templated MSNs

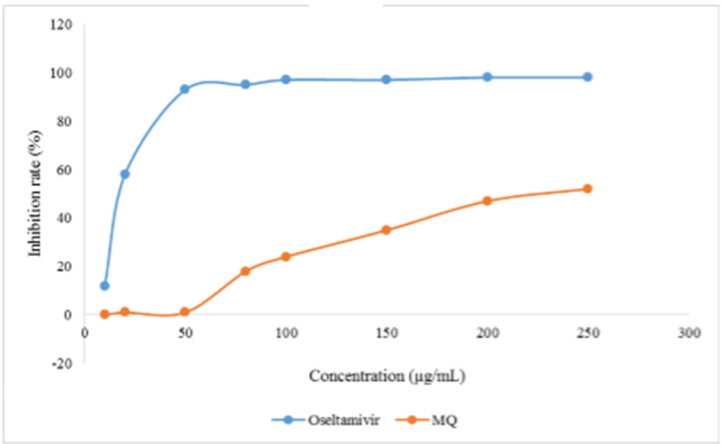


Fig. 8: Antiviral effect of QU-templated MSNs

QU in MSNs because the antioxidant effects of QU might not only shield the oxidation of MSNs but might also contribute to the antibacterial effect. Toxicity substantially impaired the additional efficacy of the nano-medicine within the biomedical field. According to Fig. 7, QU-templated MSNs are significantly biocompatible and non-toxic in different concentrations of 25, 50, 75, 100, 125, 150, 175, and 200 mg/mL in different time periods of 24, 48, and 72 h. Cell culture survival did not change significantly, and QU-templated MSNs showed tremendous biocompatibility properties. In the realm of biomedicine, these nanoparticles exhibit remarkable potential attributed to their high levels of biocompatibility and the absence of toxic side effects. Additionally, they are capable of effectively loading and transporting a variety of pharmaceutical and biological substances.

Oseltamivir is an antiviral drug applied to treatment and inhibition of influenza B and influenza A. It tends to make health problems less painful and reduce healing time by 1 to 2 days. As shown in Fig. 8, with the increase in the concentration of this drug against the viral cell population, the percentage of inhibition increases significantly. When the concentration level is raised, QU-templated MSNs eventually exhibit

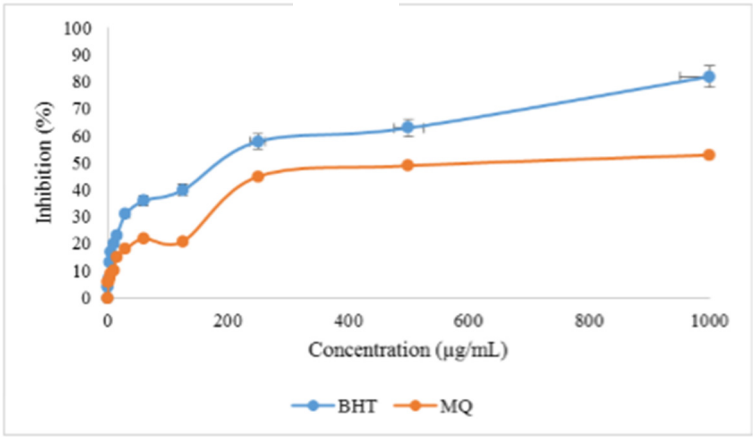


Fig. 9: Antioxidant activity of QU-templated MSNs

inhibitory effects against viral agents and have antiviral and inhibitory effects similar to those of Oseltamivir (Fig. 8).

In the Anti-DPPH assay, QU-templated MSNs, similar to BHT, show strong anti-radical effects by increasing their concentration and can provide remarkable therapeutic capacity in various clinical applications (Fig. 9).

The complete morphologic mechanism of MSNs synthesized by polyphenols (tannic acid, quercetin, Gallic acid, ethyl gallate, and eudesmic acid) was investigated. Lou *et al* reported that polyphenols have different behavior on the final size of nanoparticles regarding protein kinase A (pKa); therefore, the lower pKa leads to the synthesis of magnificent MSNs. It seems that the presence of functional groups has a key role in growing nanoparticles. To this aim, QU is able to interact with hydrogen bonds (Luo *et al.,* 2019). Naturally occurring silica, especially present in agricultural residues, serves as an alternative source for the expensive commercial silica precursors required for the synthesis of MSNs. Rice husk, a byproduct of agriculture, is most often used to produce valuable derivatives and silica goods (Pode, 2016). Another important crop grown worldwide is maize, which produces 785 million tonnes of biomass annually, with more than 60% of the biomass being silica (Kumar *et al.,* 2010). Usgodaarachchi *et al.* used the sol-gel technique to create amorphous silica mesoporous nanoparticles 50–60 nm in high purity from rice husks (Usgodaarachchi *et al.,* 2021). Porrang *et al.* (2021) created MSNs from natural sources such as rice husks and wheat. Porous silica nanoparticles are innovative sources of pharmaceuticals and have been employed as carriers of different drugs to treat different types of cancer, lessen medication toxicity, and deliver the drug to a particular site of action while still affecting other parts of the body (He *et al.,* 2020). Other applications for silica mesoporous nanoparticles include vascular tissue engineering (Shokry *et al.,* 2015), wound healing and antibacterial activities (Chen *et al.,* 2021), stem cell research (Rosenbrand *et al.,* 2018; Vafa *et al.,* 2021), and stem cell labeling (Rosenbrand *et al.,* 2018). Although antioxidant chemicals are essential for the management or prevention of many acute illnesses, including cancer, scientists face significant challenges because of their extreme instability and solubility. Then, The choice of an effective carrier can contribute to the stability of the circulatory system while minimizing unwanted interactions (Vafa and Bazargan-Lari, 2021). The salient bioavailability of MSNs makes them suitable to medical applications as potential carriers (Iraji *et al.,* 2015).

CONCLUSION

The study results revealed the mechanism by which QU forms a macromolecular framework anchored to silica, serving as a template for MSNP formulation. QU's structure results in irregular pore spaces. Using small-angle x-ray scattering, detailed data was acquired on the constituents, particularly the porous nature of the resulting MSNs. For the first time, the particle dimensions and pore formation

are regulated by the macromolecular structure of the templates. The role of QU in the morphogenetic function of MSNs has been extensively investigated, with characterization performed using TEM, SEM, XPS, XRD, and BET methods. The findings indicate that the inclusion of QU leads to a gradual increase in crystallite size, especially compared to non-mesoporous nanostructures. The QU supramolecular framework acts as a scaffold for silica precursors to polymerize around, creating pores. In addition, the production of QU-templated mesoporous silica nanostructures (QU-MSNs) were shown to possess specific pore morphology, large pore diameters, and relatively small average particle sizes. QU served as a non-surfactant, neutral template in an ammonia and ethanol mixture, resulting in approximately spherical particles with monodisperse diameters of about 180 nm. The preparation of QU-MSNs offers numerous advantages over traditional MSNs. n contrast to conventional surfactant templates, QU is characterized by its safety and non-toxic nature, making it especially advantageous for use in biomedical applications. For large-scale manufacturing, it is preferable to use a straightforward one-pot synthesis using a cheap and abundant template that can be easily extracted with water. Furthermore, the findings indicated that QU-templated MSNs exhibit inhibitory and antimicrobial activities comparable to Oseltamivir, showing increased inhibitory effects on microbial agents with higher concentrations. Like BHT, QU-templated MSNs demonstrate significant antioxidant effects when their concentration is increased and also show exceptional therapeutic potential in various clinical applications. Overall, QU-templated MSNs represent a unique type of mesoporous silica nanomaterial characterized by uniform scale, unique structure, small dimensions, and high mesoporosity, making them ideal for encapsulating biomacromolecules and drug delivery systems. The findings contribute to the development of QU-MSNs for relevant biomedical applications by elucidating the morphogenetic process of MSNs through polyphenols. This sample is particularly appropriate for drug delivery applications, supported by its interconnected architecture, which has been validated through drug release and uptake experiments. The study's focus on QU as the sole morphogenetic agent may limit the generalizability of the findings to other polyphenols, potentially overlooking alternative compounds that could offer enhanced templating properties. In addition, while various characterization techniques were employed, the absence of dynamic light scattering (DLS) restricts a comprehensive understanding of the particle size distribution and stability. The reliance on in vitro assessments without accompanying in vivo studies raises questions about the nanoparticles' safety and efficacy in biological systems. Moreover, while the synthesis method's environmental benefits are underscored, a thorough life-cycle assessment is necessary to completely understand the ecological effects of these nanoparticles throughout their lifecycle. Future research should investigate a broader range of polyphenols and natural compounds to identify additional effective morphogenetic agents for synthesizing mesoporous silica nanoparticles. Conducting in vivo studies will be essential to validate the therapeutic potential and biocompatibility of QU-templated nanoparticles, providing insights into their pharmacokinetics and safety in living organisms. Furthermore, clarifying the molecular mechanisms that regulate the interaction between QU and silica precursors will deepen our understanding and may improve the synthesis process. Finally, optimizing synthesis conditions, such as pH and temperature, could lead to nanoparticles with improved properties, enhancing their effectiveness in drug delivery applications.

AUTHOR CONTRIBUTIONS

A. Zare Hoseinabadi performed formal analysis, data acquisition, investigation, visualization, and writing original draft preparation. E. Rafiei Taqanaki performed formal analysis, data acquisition, investigation, visualization, and writing original draft preparation. A.M. Amani performed Conceptualization, Methodology, Supervision, Writing, reviewing and editing. S. Hafez Ghoran performed Conceptualization, Methodology, Supervision, Writing, reviewing and editing. H. Kamyab performed the experiments and literature review, compiled the data and manuscript preparation. A. Razmfarsa performed the experiments and literature review, compiled the data and manuscript preparation. E. Khalili performed formal analysis, data acquisition, investigation and visualization. M. Yusuf performed formal analysis, data acquisition, investigation and visualization. S. Rajendran performed formal analysis, data acquisition, investigation and visualization. All

authors read and approved the final version of the manuscript.

ACKNOWLEDGEMENT

The authors wish to thank Shiraz University of Medical Sciences for the technical support of this study. Also, the researcher extends gratitude to the Kavir Group Pty Ltd for their invaluable support and collaboration as a research support executive, contributing significantly to the success of this research.

CONFLICT OF INTEREST

The authors declare no potential conflict of interest regarding the publication of this work. In addition, the ethical issues including plagiarism, informed consent, misconduct, data fabrication and, or falsification, double publication and, or submission, and redundancy have been completely witnessed by the authors.

OPEN ACCESS

©2024 The author(s). This article is licensed under a Creative Commons Attribution 4.0 International License, which permits use, sharing, adaptation, distribution and reproduction in any medium or format, if you give appropriate credit to the original author(s) and the source, provide a link to the Creative Commons license, and indicate if changes were made. The images or other third-party material in this article are included in the article's Creative Commons license, unless indicated otherwise in a credit line to the material., If material is not included in the article's Creative Commons license and your intended use is not permitted by statutory regulation or exceeds the permitted use, you will need to obtain permission directly from the copyright holder. To view a copy of this license, visit:

http://creativecommons.org/licenses/by/4.0/

PUBLISHER'S NOTE

GJESM Publisher remains neutral with regard to jurisdictional claims in published maps and institutional affiliations.

ABBREVIATIONS

%	Percentage value
°C	Degree Celsius
ANOVA	*Analysis of variance*
Au	*Gold*
BET	Brunauer–emmett teller
BHT	Butylated hydroxytoluene
BJH	Barrett-joyner-halenda
C	*Carbon*
CFU	*Colonogenic cell numbers*
CLSI	Clinical and laboratory standard institute
CTAB	Cetyltrimethylammonium bromide
DPPH	2,2-diphenyl-1-picrylhydrazyl
EDS and EDX	Energy-dispersive X-ray spectroscopy
EDS and EDX	Energy-dispersive X-ray spectroscopy
FCC	Face center cubic
Fe	*Iron*
FT-IR	Fourier transform infrared
g	Gram
H_2O_2	Hydrogen peroxide
h	Hour
LB	Lactose broth
MBC	Minimum bactericidal concentration
CFU	McFarland's standard
Mg/mL	Microgram per milliliter
MIC	Minimum inhibitory concentration
mL	Milliliters
MSNs	Mesoporous silica nanoparticles
MTT	*3-4, 5-dimethylthiazolyl-2-2, 5-diphenyltetrazolium bromide*
N	*Nitrogen*
Na_2CO_3	*Sodium carbonate*

NB	Nutrient broth
O	Oxygen
PBS	Phosphate-buffered saline
pH	Potential of hydrogen
PKa	*Protein kinase A*
QU	Quercetin
rpm	Revolutions per minute
SAXS	Small angle x-ray scattering
SEM	Scanning electron microscopy
SPSS	Social Sciences Statistics Package
Si	*Silicon*
TEM	Transmission electron microscopy
TEOS	Tetraethoxysilane
WAXRD	Wide-angle X-ray diffraction
XPS	X-ray photoelectron spectroscopy
XRD	X-ray diffraction analysis
Zn	*Zinc*

REFERENCES

Abbas, M.; Saeed, F.; Anjum, F.M.; Afzaal, M.; Tufail, T.; Bashir, M. S.; Suleria, H.A.R., (2017). Natural polyphenols: An overview. Int. J. Food Prop., 20: 1689-1699 **(11 pages).**

Sarkar, A.; Ghosh, S.; Chowdhury, S.; Pandey, B.; Sil, P.C., (2016). Targeted delivery of quercetin loaded mesoporous silica nanoparticles to the breast cancer cells. Biochim. Biophys., Acta (BBA)-General Subjects. 1860: 2065-2075 **(11 pages).**

Amani, A.M.; Tayebi, L.; Vafa, E.; Abbasi, M.; Vaez, A.; Kamyab, H.; Bazargan-Lari, R., (2024). On the horizon of greener pathways to travel into a greener future portal: Green MXenes, environment-friendly synthesis, and their innovative applications. J. Cleaner Prod., 140606 **(23 pages).**

Balouiri, M.; Sadiki, M.; Ibnsouda, S.K., (2016). Methods for in vitro evaluating antimicrobial activity: A review. J. Pharm. Anal., 6: 71-79 **(9 pages).**

Chen, J.; Qiu, L.; Li, Q.; Ai, J.; Liu, H.; Chen, Q., (2021). Rapid hemostasis accompanied by antibacterial action of calcium crosslinking tannic acid-coated mesoporous silica/silver Janus nanoparticles. Mater. Sci. Eng., 123: 111958 **(8 pages).**

David, A.V.A.; Arulmoli, R.; Parasuraman, S., (2016). Overviews of biological importance of quercetin: A bioactive flavonoid. Pharmacogn. Rev., 10: 84 **(11 pages).**

Fröba, M.; Köhn, R.; Bouffaud, G.; Richard, O.; van Tendeloo, G., (1999). Fe2O3 nanoparticles within mesoporous MCM-48 silica: in situ formation and characterization. Chem. Mater., 11: 2858-2865 **(8 pages).**

Gao, Z.; Zharov, I., (2014). Large pore mesoporous silica nanoparticles by templating with a nonsurfactant molecule, tannic acid. Chem. Mater., 26: 2030-2037 **(8 pages).**

Ghoran, S.H.; Firuzi, O.; Jassbi, A.R., (2020). Phytoconstituents from the aerial parts of Salvia dracocephaloides Boiss. and their biological activities. J. Env. Treat. Tech., 8: 1274-1278 **(5 pages).**

Han, L.; Che, S., (2013). Anionic surfactant templated mesoporous silicas (AMSs). Chem. Soc. Rev., 42: 3740-3752 **(12 pages).**

He, Y.; Shao, L.; Usman, I.; Hu, Y.; Pan, A.; Liang, S.; Xu, H., (2020). A pH-responsive dissociable mesoporous silica-based nanoplatform enabling efficient dual-drug co-delivery and rapid clearance for cancer therapy. Biomater. Sci., 8: 3418-3429 **(12 pages).**

Iraji, S.; Rashidi, L.; Ganji, F., (2015). Functionalized Mesoporous silica nanoparticles as a novel antioxidant delivery system. Iran J. Chem. Eng., 12: 93 **(11 pages).**

Kioni, P.N.; Gao, Y.; Tang, Z.; Gatebe, E.; Wanyika, H., (2011). Synthesis and characterization of ordered mesoporous silica nanoparticles with tunable physical properties by varying molar composition of reagents. **(9 pages).**

Kumar, S.; Upadhyaya, J.S.; Negi, Y.S., (2010). Preparation of nanoparticles from corn cobs by chemical treatment methods. BioResources. 5: 1292-1300 **(9 pages).**

Lakhanpal, P.; Rai, D.K., (2007). Quercetin: a versatile flavonoid., Int. J. Med. Update. 2: 22-37 **(16 pages).**

Loizzo, M.R.; Tundis, R.; Bonesi, M.; Menichini, F.; De Luca, D.; Colica, C.; Menichini, F., (2012). Evaluation of Citrus aurantifolia peel and leaves extracts for their chemical composition, antioxidant and anti-cholinesterase activities. J. Sci. Food Agric., 92: 2960-2967 **(8 pages).**

Luo, J.; Panzarasa, G.; Osypova, A.; Sorin, F.; Spano, F.; Rossi, R.M.; Boesel, L.F., (2019). Polyphenols as morphogenetic agents for the controlled synthesis of mesoporous silica nanoparticles. Chem. Mater., 31: 3192-3200 **(9 pages).**

Maldonado, M.; Carmona, M.C.; Velásquez, Z.; Puig, A.; Cruzado, A.; López, A.; Young, C.M., (2005). Siliceous sponges as a silicon sink: an overlooked aspect of benthopelagic coupling in the marine silicon cycle.

Limnol. Oceanogr., 50: 799-809 **(11 pages).**

Matshitse, R., (2010). Brunauer-Emmett-Teller (BET) surface area analysis. Rhodes Univ. Natl. Res. Found., 384 **(7 pages).**

Nikolić, M.; Giannakopoulos, K.P.; Srdić, V.V., (2010). Synthesis and characterization of mesoporous silica core-shell particles. Process. Appl. Ceram., 4: 81-85 **(5 pages).**

Pang, J. B.; Qiu, K.Y.; Wei, Y., (2001). A new nonsurfactant pathway to mesoporous silica materials based on tartaric acid in conjunction with metallic chloride. Chem. Mater., 13: 2361-2365 **(5 pages).**

Pang, J.B.; Qiu, K. Y.; Wei, Y., (2001). Preparation of mesoporous silica materials with non-surfactant hydroxy-carboxylic acid compounds as templates via sol–gel process. J. Non-Cryst. Solids, 283: 101-108 **(8 pages).**

Pode, R., (2016). Potential applications of rice husk ash waste from rice husk biomass power plant. Renew. Sustainable Energy Rev., 53: 1468-1485 **(18 pages).**

Porrang, S.; Rahemi, N.; Davaran, S.; Mahdavi, M.; Hassanzadeh, B., (2021). Preparation and in-vitro evaluation of mesoporous biogenic silica nanoparticles obtained from rice and wheat husk as a biocompatible carrier for anti-cancer drug delivery. Eur. J. Pharm. Sci., 163: 105866 **(8 pages).**

Riesgo, A.; Taboada, S.; Kenny, N.J.; Santodomingo, N.; Moles, J.; Leiva, C.; Maldonado, M., (2021). Recycling resources: silica of diatom frustules as a source for spicule building in Antarctic siliceous demosponges. Zool. J. Linn. Soc., 192: 259-276 **(18 pages).**

Rosenbrand, R.; Barata, D.; Sutthavas, P.; Mohren, R.; Cillero-Pastor, B.; Habibovic, P.; van Rijt, S., (2018). Lipid surface modifications increase mesoporous silica nanoparticle labeling properties in mesenchymal stem cells. Int. J. Nanomed., 7711-7725 **(15 pages).**

Sarkar, A.; Ghosh, S.; Chowdhury, S.; Pandey, B.; Sil, P.C., (2016). Targeted delivery of quercetin loaded mesoporous silica nanoparticles to the breast cancer cells. Biochim. Biophys. Acta. Biophys., (BBA)-General Subjects. 1860: 2065-2075 **(11 pages).**

Shokry, H.; Vanamo, U.; Wiltschka, O.; Niinimäki, J.; Lerche, M.; Levon, K.; Sahlgren, C., (2015). Mesoporous silica particle-PLA–PANI hybrid scaffolds for cell-directed intracellular drug delivery and tissue vascularization. Nanoscale. 7: 14434-14443 **(10 pages).**

Stevens, W.J.; Lebeau, K.; Mertens, M.; Van Tendeloo, G.; Cool, P.; Vansant, E.F., (2006). Investigation of the morphology of the mesoporous SBA-16 and SBA-15 materials. J. Phys. Chem., 110: 9183-9187 **(5 pages).**

Twentyman, P.R.; Luscombe, M., (1987). A study of some variables in a tetrazolium dye (MTT) based assay for cell growth and chemosensitivity. Br. J. Cancer, 56: 279-285 **(7 pages).**

Usgodaarachchi, L.; Thambiliyagodage, C.; Wijesekera, R.; Bakker, M.G., (2021). Synthesis of mesoporous silica nanoparticles derived from rice husk and surface-controlled amine functionalization for efficient adsorption of methylene blue from aqueous solution. Curr. Res. Green Sustainable Chem., 4: 100116 **(11 pages).**

Vafa, E.; Azizli, M.J.; Tayebi, L.; Amani, A.M.; Kamyab, H., (2024). Integrating bioactive glass with compatibilizer: a novel approach for hard tissue regeneration using PXDDA-co-PLA/PLCL/PGLA nanocomposites. Mater. Chem. Phys., 316: 129070 **(9 pages).**

Vafa, E.; Bazargan-Lari, R., (2021). Bovine serum albumin protected gold nanozymes as a novel anti-cancer nanodrug for acute T-type lymphoblastic leukemia treatment via effect on the expression of anti-apoptotic genes. Appl. Biol. Chem., 64: 86 **(10 pages).**

Vafa, E.; Bazargan-Lari, R.; Bahrololoom, M.E., (2021). Synthesis of 45S5 bioactive glass-ceramic using the sol-gel method, catalyzed by low concentration acetic acid extracted from homemade vinegar. J. Mater. Res. Technol., 10: 1427-1436 **(9 pages).**

Vafa, E.; Tayebi, L.; Abbasi, M.; Azizli, M.J.; Bazargan-Lari, R.; Talaiekhozani, A.; Chelliapan, S., (2023). A better roadmap for designing novel bioactive glasses: effective approaches for the development of innovative revolutionary bioglasses for future biomedical applications. Environ. Sci. Pollut. Res., 30: 116960-116983 **(24 pages).**

Wei, Y.; Jin, D.; Ding, T.; Shih, W.H.; Liu, X.; Cheng, S.Z.; Fu, Q., (1998). A non-surfactant templating route to mesoporous silica materials. Adv. Mater., 10: 313-316 **(4 pages).**

Wei, Y.; Xu, J.; Dong, H.; Dong, J.H.; Qiu, K.; Jansen-Varnum, S.A., (1999). Preparation and physisorption characterization of d-glucose-templated mesoporous silica sol–gel materials. Chem. Mater., 11: 2023-2029 **(7 pages).**

Xu, Y.; Xu, S.; Emmler, T.; Roelofs, F.; Boettcher, C.; Haag, R.; Buntkowsky, G., (2008). A novel green template for the synthesis of mesoporous silica. Chem. Eur. J., 14: 3311-3315 **(5 pages).**

Zhao, D.; Feng, J.; Huo, Q.; Melosh, N.; Fredrickson, G.H.; Chmelka, B.F., Stucky, G.D., (1998). Triblock copolymer syntheses mesoporous silica with periodic 50 to 300 angstrom pores. science, 279: 548-552 **(5 pages).**

Zheng, J.Y.; Pang, J.B.; Qiu, K.Y.; Wei, Y., (2002). Synthesis of mesoporous silica materials via nonsurfactant templated sol-gel route by using mixture of organic compounds as template. J. Sol-Gel. Sci. Technol., 24: 81-88 **(8 pages).**

AUTHOR (S) BIOSKETCHES

Zare Hoseinabadi, A.R., Ph.D., Assistant Professor, Department of Medical Nanotechnology, School of Advanced Medical Sciences and Technologies, Shiraz University of Medical Sciences, Shiraz, Iran
- Email: *ar.zare00@gmail.com*
- ORCID: 0000 0001 7297 8065
- Web of Science ResearcherID: ADX-2248-2022
- Scopus Author ID: 55795600300
- Homepage: https://scholar.google.com/citations?user=8hgcHPUAAAAJ&hl=en

Rafiei Taqanaki , E., Ph.D., Assistant Professor, Department of Medical Nanotechnology, School of Advanced Medical Sciences and Technologies, Shiraz University of Medical Sciences, Shiraz, Iran
- Email: *erafie@rocketmail.com*
- ORCID: 0000-0002-3061-9758
- Web of Science ResearcherID: IZP-6822-2023
- Scopus Author ID: 55468022900
- Homepage: https://scholar.google.com/citations?user=JzBtDRYAAAAJ&hl=en

Hafez Ghoran, S., Ph.D. Candidate, Department of Medical Nanotechnology, School of Advanced Medical Sciences and Technologies, Shiraz University of Medical Sciences, Shiraz, Iran.
- Email: *s_Hafezghoran@yahoo.com*
- ORCID: 0000-0002-3061-9754
- Web of Science ResearcherID: ABD-9876-2020
- Scopus Author ID: 57195483722
- Homepage: https://www.webofscience.com/wos/author/record/2122428

Amani, A.M., Ph.D., Associate Professor, Department of Medical Nanotechnology, School of Advanced Medical Sciences and Technologies, Shiraz University of Medical Sciences, Shiraz, Iran
- Email: *amani_a@sums.ac.ir*
- ORCID: 0000-0002-5965-1575
- Web of Science ResearcherID: AAP-1567-2021
- Scopus Author ID: 56355136200
- Homepage: https://typeset.io/authors/ali-mohammad-amani-2he5flobw5

Kamyab, H., Ph.D., Assistant Professor, [1]Faculty of Chemical and Energy Engineering, Universiti Teknologi Malaysia, 81310, Skudai, Johor, Malaysia. [2]Universidad UTE, Centro de Investigación en Salud Públicay Epidemiología Clínica (CISPEC), Quito 170527, Ecuador. [3]Department of Biomaterials, Saveetha Dental College, and Hospital, Saveetha Institute of Medical and Technical Sciences, Chennai, 600 077, India.
- Email: *hesam_kamyab@yahoo.com*
- ORCID: 0000-0002-5272-2297
- Web of Science ResearcherID: H-4583-2016
- Scopus Author ID: 55355146400
- Homepage: https://www.webofscience.com/wos/author/record/H-4583-2016

Razmfarsa, **S.,** Ph.D. Candidate, Faculty of Science, Department of Biology and Genetics, Islamic Azad University, Mashhad Branch, Razavi Khorasan, Iran
- Email: *razmfarsaatoosa@gmail.com*
- ORCID: 0009-0009-0535-6464
- Web of Science ResearcherID: SD-9676-2023
- Scopus Author ID: 60105149
- Homepage: https://www.linkedin.com/in/atoosa-razmfarsa-2445a3328/?originalSubdomain=ir

Khalili, E., Ph.D., Assistant Professor, Department of Electrical and Engineering, Faculty of Engineering and Physical Science, Centre of Vision Speech and Processing, University of Surrey, United Kingdom
- Email: elhambakhtiari1986@gmail.com
- ORCID: 0000-0002-7955-7068
- Web of Science ResearcherID: G-8333-2019
- Scopus Author ID: 56845475300
- Homepage: https://scholar.google.com/citations?user=iWm-jkEAAAAJ&hl=en

Yusuf, M., Ph.D., Assistant Professor, Clean Energy Technologies Research Institute, Process Systems Engineering, Faculty of Engineering and Applied Science, University of Regina, Canada
Centre of Research Impact and Outcome, Chitkara University Institute of Engineering and Technology, Chitkara University, Punjab, India
- Email: *mohd.yusuf@uregina.ca*
- ORCID: 0000-0003-2442-5161
- Web of Science ResearcherID: AAY-2977-2021
- Scopus Author ID: 57220490203
- Homepage: https://www.linkedin.com/in/dr-mohammad-yusuf-3a4b9397?utm_source=share&utm_campaign=share_via&utm_content=profile&utm_medium=android_app

AUTHOR (S) BIOSKETCHES

Rajendran, S., Ph.D., Professor, Institute de Alta Investigación, Universidad de Tarapacá, Arica 1000000, Chile.
- Email: *saravanan3.raj@gmail.com*
- ORCID: 0000-0002-3771-4694
- Web of Science ResearcherID: J-3287-2014
- Scopus Author ID: 7004886581
- Homepage: https://www.webofscience.com/wos/author/record/1203114

HOW TO CITE THIS ARTICLE

Zare Hoseinabadi, A.R.; Rafiei Taqanaki, E.; Hafez Ghoran, S.; Amani, A.M.; Kamyab, H.; Razmfarsa, A.; Khalili, E.; Yusuf, M.; Rajendran, S., (2024). Environmentally friendly synthesis of nanoporous silica materials using quercetin as a morphogenetic agent. Global J. Environ. Sci. Manage., 10(SI): 137-152.

DOI: 10.22034/gjesm.2024.10.SI.09

URL: https://www.gjesm.net/article_716241.html